The Relationship Between Insertion Angles, Default Frequency Allocations, and Spiral Ganglion Place Pitch in Cochlear Implants

David M. Landsberger, Maja Svrakic, J. Thomas Roland, Jr., and Mario Svirsky

Objectives: Commercially available cochlear implant systems attempt to deliver frequency information going down to a few hundred Hertz, but the electrode arrays are not designed to reach the most apical regions of the cochlea, which correspond to these low frequencies. This may cause a mismatch between the frequencies presented by a cochlear implant electrode array and the frequencies represented at the corresponding location in a normal-hearing cochlea. In the following study, the mismatch between the frequency presented at a given cochlear angle and the frequency expected by an acoustic hearing ear at the corresponding angle is examined for the cochlear implant systems that are most commonly used in the United States.

Design: The angular insertion of each of the electrodes on four different electrode arrays (MED-EL Standard, MED-EL Flex28, Advanced Bionics HiFocus 1J, and Cochlear Contour Advance) was estimated from X-ray. For the angular location of each electrode on each electrode array, the predicted spiral ganglion frequency was estimated. The predicted spiral ganglion frequency was compared with the center frequency provided by the corresponding electrode using the manufacturer's default frequency-to-electrode allocation.

Results: Differences across devices were observed for the place of stimulation for frequencies below 650 Hz. Longer electrode arrays (i.e., the MED-EL Standard and Flex28) demonstrated smaller deviations from the spiral ganglion map than the other electrode arrays. For insertion angles up to approximately 270°, the frequencies presented at a given location were typically approximately an octave below what would be expected by a spiral ganglion frequency map, while the deviations were larger for angles deeper than 270°. For frequencies above 650 Hz, the frequency to angle relationship was consistent across all four electrode models.

Conclusions: A mismatch was observed between the predicted frequency and the default frequency provided by every electrode on all electrode arrays. The mismatch can be reduced by changing the default frequency allocations, inserting electrodes deeper into the cochlea, or allowing cochlear implant users to adapt to the mismatch. Further studies are required to fully assess the clinical significance of the frequency mismatch.

Key words: Frequency allocation, Insertion depth, Place pitch, Spiral ganglion.

(Ear & Hearing 2015;36;e207–e213)

INTRODUCTION

Cochlear implants (CIs) depend on the tonotopic organization of the cochlea to provide frequency information. CIs have arrays of electrodes inserted into the cochlea. With typical CI sound coding, each electrode on the array is assigned a frequency range in an attempt to mimic the tonotopicity of the normal auditory system. Low acoustic frequencies are presented on the more deeply inserted electrodes and therefore sound lower in pitch to a CI user than high acoustic frequencies, which are presented on the more basal electrodes. The default center frequencies for the most apical and basal electrodes vary across CI manufacturers (242 Hz and 7421 Hz for Cochlear, 322 Hz and 6346 Hz for Advanced Bionics, and 149 Hz and 7412 Hz for MED-EL FSP/FS4 strategies). However, because none of the commercially available electrode arrays are designed to reach the most apical regions of the cochlea, there is likely to be a mismatch between the cochlear location stimulated by an implant in response to a given frequency and the location stimulated by the same frequency in a normal cochlea. This may not be an issue for prelingually deaf CI users who develop speech perception based exclusively on input provided by the implant. However, frequency mismatch may be a problem for CI users who learned to understand speech based on the normal frequency-to-place function, then lost their hearing, and after receiving an implant have to adapt to a new and potentially different frequency-to-place function. A function to estimate the frequency that is represented at a given basilar membrane location by a normal ear has been developed by Greenwood (1961) and further modified by Stakhovskya et al. (2007) to account for spiral ganglion neuron location, which is considered the most likely site for CI stimulation.

The ramifications of the place pitch mismatch provided by a CI are unclear. With CI experience, the auditory system adapts such that the pitch associated with a given electrode location shifts toward the frequency information provided by the CI at that location (Svirsky et al. 2004; Reiss et al. 2007, 2014). Similarly, sound quality with a CI also shifts with time. Patients often describe the sound quality of speech as high pitched, robotic, and "Donald Duck"-like when first activated. Numerous anecdotal reports indicate that after experience with the implant, the sound quality from the implant becomes "normal" or at least more normal. These longitudinal changes are accompanied by improvements in speech perception. Although it is widely accepted that most improvement in speech perception performance is seen in the first 3 to 6 months of implant use for postlingual CI recipients, in some cases it might take months or even years to reach asymptotic levels (e.g., Tyler et al. 1997; Svirsky et al. 2001; Hamzavi et al. 2003; Ruffin et al. 2007; Holden et al. 2013). CI simulations have shown that in acute situations (i.e., with no opportunity for plasticity), listeners can generally tolerate a ±3 mm shift in place of stimulation with only small decrements in speech perception (Fu & Shannon 1999; Li & Fu 2010), suggesting that proper place pitch matches might not be critical for basic speech understanding. Nevertheless, deviations from the natural frequency locations might limit performance, increase the amount of time postactivation for a CI

Department of Otolaryngology, New York University School of Medicine, New York, USA.

user to reach asymptote performance, and reduce sound quality (Hochmair et al. 2003; Başkent & Shannon 2003, 2005; Fitzgerald et al. 2008; Buchman et al. 2014). For example, recent data (Buchman et al. 2014) suggest that users of a 31-mm electrode array (MED-EL Standard) perform better and reach asymptotic performance faster than users of a 24-mm electrode array (M), although this small study failed to reach significance ($p = 0.07$). The ideal electrode length, insertion depth, and frequency allocation are still under discussion in the literature, and it is at least possible that a single setting of all these design parameters may not be ideal for all listeners. In any case, it seems clear that electrode length, position, and the frequencies assigned to each electrode contact have a significant influence on speech perception, sound quality, and ease of adaptation to the CI.

In the present article, we examined the placement of multiple different CI electrode arrays from the patient population at the New York University Cochlear Implant Center. Specifically, we measured the range (in degrees) between the most apical and the most basal electrodes in the array from X-rays. In addition, for each electrode location, we compared the default frequency assigned to the location with the frequency predicted to be represented in the cochlea by a normal acoustic ear according to the spiral ganglion place-frequency map derived by Stakhovskaya et al. (2007). The following data provide insight into the cochlear range represented by four different electrode arrays, as well as the potential frequency mismatches typically presented to a CI user.

METHODS

Subjects

X-rays for 92 ears with CIs from the New York University Cochlear Implant Center were examined. Thirteen ears were implanted with the MED-EL Standard electrode array, five ears were implanted with the MED-EL Flex28 electrode array, 30 ears were implanted with the Advanced Bionics HiFocus 1J electrode array, and 44 ears were implanted with the Cochlear Nucleus Contour Advance electrode array.

Surgical Technique

A single surgeon implanted 75% of the electrode arrays, and two surgeons implanted 89% of them. All surgeries were performed using the standard transmastoid, transfacial recess (posterior tympanotomy) approach to the cochlea. A peri-round window (RW) cochleostomy was used for access. This is accomplished by carefully drilling away bone just inferior to the RW approaching the floor of the scala tympani. Once the endosteum is encountered, it is carefully opened without suctioning the perilymph. In some cases, 50% dilute glycerin solution is applied over the cochleostomy so that blood and bone dust floats away from the cochleostomy site. The endosteum is carefully opened, and the electrode is inserted to its distal mark. The electrode is then advanced (off the stylet in the case of Advanced Bionics 1J and Cochlear Contour Advance electrodes) either with the insertion tool supplied by the manufacturer or with a manual technique until a full insertion is obtained. Full insertion is determined by the insertional (proximal) stop point on the electrode lead. The tool and/or stylet are disengaged. The cochleostomy is then sealed using previously harvested small strips of periosteum. Intraoperative impedances and electrically evoked compound action potentials confirm a functional device.

An intraoperative plain X-ray is taken using a transorbital view for simultaneous bilateral implants and an anti-Stenver's view (head tilted at 30 to 45 degrees away from the operated side—see Fig. 1) for unilateral implants. The X-ray beam is directed perpendicular to the plane of the operating table, which is leveled before obtaining the image. The image is obtained to verify intracochlear placement and rule out tip rollover or electrode kinks that could be corrected before awakening the patient from general anesthesia. A digital copy of the film is saved in the patient record. A study of 288 surgeries using Nucleus CIs done at our institution (Cosetti et al. 2012) showed five instances of

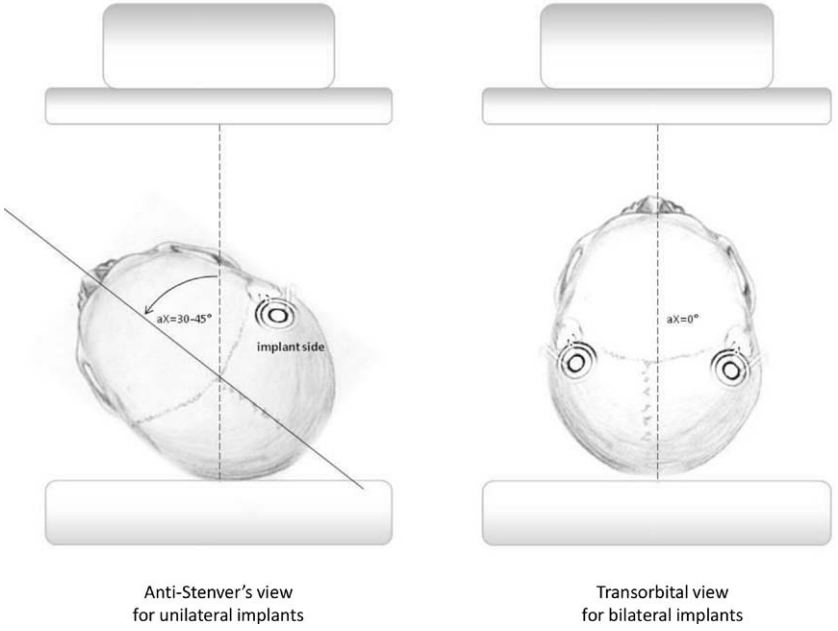

Fig. 1. Angle of head rotation relative to X-ray beam. aX indicates angle of X-ray.

tip rollover or extracochlear electrode placement, which were all corrected after being detected in the intraoperative X-ray.

Measurement of Angular Depth of Insertion

Angular depth of insertion (aDOI) was measured based on an earlier described method (Marsh et al. 1993; Cohen et al. 1996; Xu et al. 2000). Two reference lines are drawn on the two-dimensional radiograph images. The first reference line is a vertical through the apex of the superior semicircular canal and the center of the vestibule; the point where this line intersects the electrode lead approximates the RW. The second reference line passes through the RW point and a modiolus point. The modiolus point is determined as the approximate center of the electrode spiral as it sits in the cochlea (see Fig. 2). This second reference line is 0° rotation; each electrode point can be calculated as the angle of rotation it assumes from the 0° reference line. The most distal electrode's angle from the 0° reference line is what was measured for aDOI. All angles were measured by converting the files to .jpg format and analyzing with free downloadable "ImageJ" software available at http://rsbweb.nih.gov/ij/download.html.

RESULTS

The insertion angle location of all electrodes for 92 cochlear implantations was calculated. The mean insertion angles for the most apical electrode for each of the four electrode array models are presented in Table 1 alongside insertion angle for the most apical electrode results from other studies. In the left panel of Figure 3, the insertion range for each ear (defined as the range in insertion angle from the most apical to the most basal electrode) is plotted in order of the position of the most apical electrode. A fair amount of variability of insertion angles both within and across electrode array types is observed. In the right panel of Figure 3, the mean insertion ranges for each electrode type are plotted. A Kruskal-Wallis one-way analysis of variance on ranks ($H_3 = 37.214$, $p < 0.001$) detected a significant difference between the insertion ranges across electrode arrays. Post hoc pairwise comparisons (Dunn method) reveal significant differences between the MED-EL Standard array and the Advanced Bionics HiFocus 1J and Nucleus Contour Advance arrays. Similarly, significant differences between the MED-EL Flex28 and the HiFocus 1J and Contour Advance arrays were observed. However, no differences were detected in the insertion range between the HiFocus 1J and the Contour Advance arrays or between the MED-EL Standard and the Flex28 arrays. A similar analysis reveals differences in the positions of the most apical electrodes in the array ($H_3 = 28.713$, $p < 0.001$). Post hoc pairwise comparisons reveal significant differences in the apical-most position between the MED-EL Standard array and both the Advanced Bionics HiFocus 1J and the Nucleus Contour Advance electrode arrays, as well as significant difference between the Flex28 and the Contour Advance arrays. A Kruskal-Wallis one-way analysis of variance on ranks ($H_3 = 21.960$, $p < 0.001$) reveals a significant difference between the basal location of the different arrays. Post hoc pairwise comparisons reveal that the HiFocus 1J basal position is significantly different than all other arrays in the basal location. The variability in the HiFocus 1J insertion could potentially be explained by the lack of a fixed insertional stop point, which may result in more variable insertion angle.

The mean locations for each electrode on each electrode array are plotted in Figure 4 as a function of the center frequency of the filter corresponding to the electrode position from the default frequency allocation table. In addition, the place-frequency map for neurons in the spiral ganglion (Stakhovskaya et al. 2007) is plotted in green. For frequencies above approximately 650 Hz, the place-frequency functions

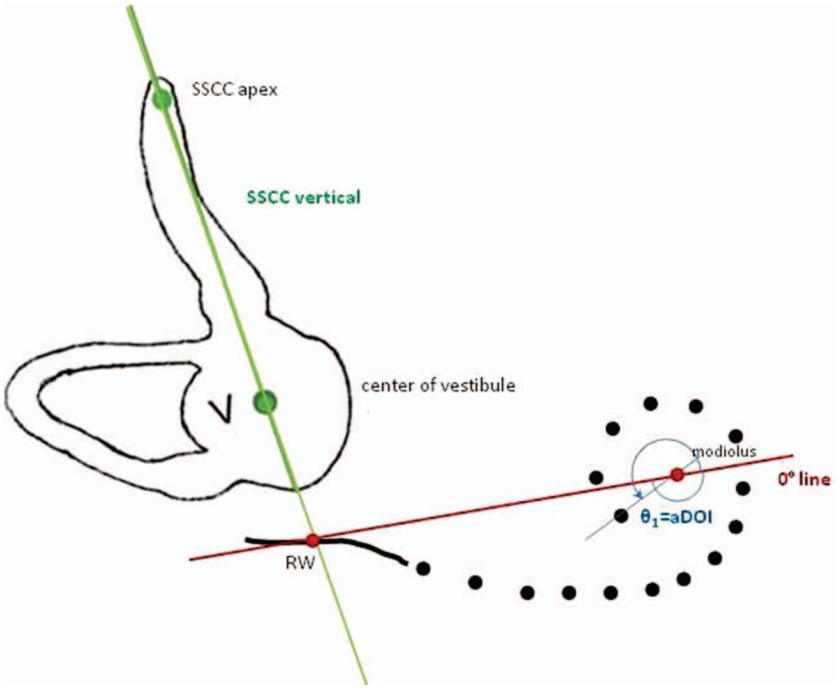

Fig. 2. Calculation of angular depth of insertion (aDOI). θ1 through θ16 represent the aDOI for electrodes 1 through 16 (in a representative 16 electrode implant) in degrees past 0° line; SSCC, superior semicircular canal; RW, round window (intersection between SSCC vertical and electrode lead); V, center of vestibule.

TABLE 1. Summary of insertion angles from multiple studies using multiple electrode arrays

Publication	Manufacturer	Electrode	n	Mean	SD	Median	Min	Max	Range
van der Marel et al. (2014)	Advanced Bionics	HiFocus 1J	362	480	68		289	678	389
Kós et al. (2005)	Advanced Bionics	HiFocus 1J	5	479	111				
Landsberger et al. (this study)	**Advanced Bionics**	**HiFocus 1J**	**30**	**405**	**78**	**391**	**257**	**584**	**327**
Holden (Reference Note 1)	Advanced Bionics	HiFocus 1J	9	382	72		297	535	238
Trieger et al. (2011)	Cochlear	Contour Advance	7	469	66		374	537	163
Holden (Reference Note 1)	Cochlear	Contour Advance	62	406	86		231	751	520
Landsberger et al. (this study)	**Cochlear**	**Contour Advance**	**44**	**381**	**51**	**375**	**267**	**494**	**227**
Fraysse et al. (2006)	Cochlear	Contour Advance	34	376	71		300	435	135
Adunka et al. (2006)	Cochlear	Contour Advance	16	357		360	180	400	220
Radeloff et al. (2008)	Cochlear	Contour Advance	18	348	42		270	405	135
Trieger et al. (2011)	MED-EL	Standard	8	700	49		605	751	146
Baumann and Nobbe (2004)	MED-EL	Standard	8	697			630	810	180
Gani et al. (2007)	MED-EL	Standard	5	670			605	720	115
Kós et al. (2005)	MED-EL	Standard	4	657	83				
Vermeire et al. (2008)	MED-EL	FlexSOFT	9	652	63	644	565	758	193
Landsberger et al. (this study)	**MED-EL**	**Standard**	**13**	**544**	**93**	**569**	**397**	**714**	**317**
Hamzavi and Arnoldner (2006)	MED-EL	Standard	8	543	20	550	510	560	50
Hamzavi and Arnoldner (2006)	MED-EL	FlexSOFT	2	540	14	540	530	550	20
Landsberger et al. (this study)	**MED-EL**	**Flex28**	**5**	**471**	**42**	**486**	**417**	**514**	**97**
Radeloff et al. (2008)	MED-EL	Standard	28	454	171		160	720	560

Units for mean, standard deviation (SD), median, minimum insertion angle (min), maximum insertion angle (max), and range of insertion angles are degrees. Results are organized by manufacturer. Within manufacturer, results are sorted by mean insertion depth for the corresponding study.

are similar for all devices. However, substantial deviations in the place-frequency functions are observed for frequencies below approximately 650 Hz. Figure 5 shows that the default frequencies provided by all four electrode arrays are approximately an octave below the predicted spiral ganglion pitch for insertions up to approximately 270°. Beyond 270°, the deviation between the default frequency and the predicted SG pitch is varied across electrode arrays. Similarly, for insertion angles below approximately 270°, a deeper insertion of approximately 90° would provide an accurate default frequency allocation to represent the predicted SG pitch for the corresponding location for all electrode arrays. However, for electrodes located beyond 270°, the deeper insertion required to maintain the SG pitch estimate increases and becomes more variable across electrode arrays.

DISCUSSION

Clearly, there are important similarities, as well as differences, among electrode location data for the four different types of electrodes, and between all electrode types and the spiral ganglion frequency versus angle of insertion function. One difference is that the MED-EL Standard and Flex28 electrode arrays are longer and achieve a deeper insertion angle than the HiFocus 1J and the Contour Advance arrays. The MED-EL Standard and Flex28 measure 31 and 28 mm in length, while the HiFocus 1J and the Contour Advance are 25 and 24 mm in length, respectively. Another significant point is that all four electrode arrays, when combined with the corresponding default frequency-to-electrode tables, result in a frequency shift of about one octave (12 semitones) with respect to the place-frequency map in the spiral

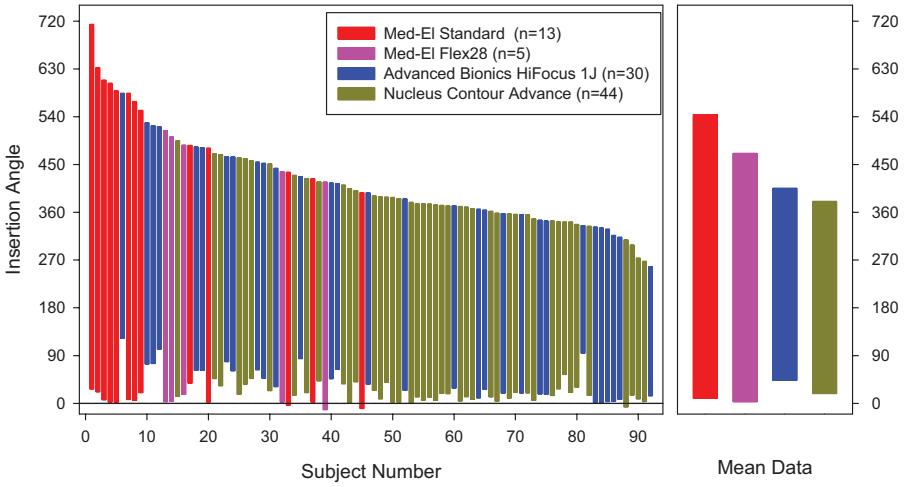

Fig. 3. Each bar represents the insertion angles for the most apical and most basal electrode. Bars are sorted from most apical insertion to least apical insertion (left). Colors of bars are coded by electrode array type. Mean insertion depths of most apical and most basal electrodes are presented for each electrode type (right).

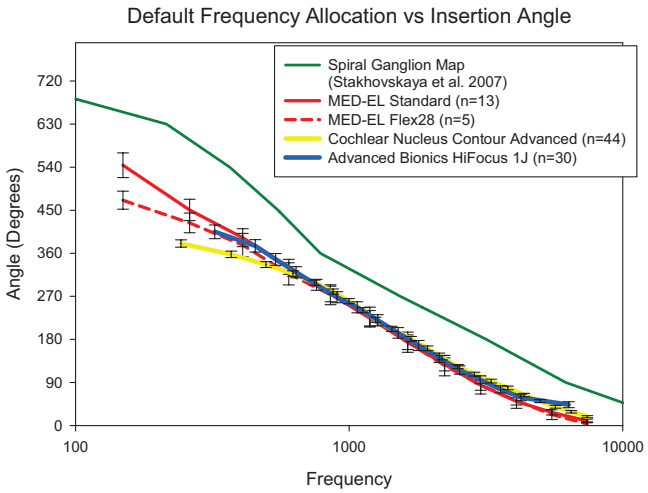

Fig. 4. Average insertion angle for each electrode array type plotted as a function of the corresponding default frequency allocated for that electrode. The estimate of spiral ganglion place pitch is plotted in green. Colors of lines are coded by electrode array type.

ganglion. It is important to note that the present results are consistent with other published studies regarding range and average angle of insertion of Cochlear and Advanced Bionics electrodes, but they do fall toward the low end of the range in the case of the two MED-EL electrode arrays (Table 1).

This type of frequency shift can be minimized in at least three ways: by using electrode arrays that reach a deeper insertion angle, by using different frequency-to-electrode tables, or by letting patients adjust to the new frequency-place map hoping that auditory plasticity will compensate for the frequency shift. Deeper insertion angles would move data points in Figure 4 upward, getting closer to the spiral ganglion map curve. Changing the frequency-to-electrode table to higher values would move points in Figure 4 from left to right, achieving the same result. Last, auditory plasticity would change the spiral ganglion map in the direction of the frequency table used by the

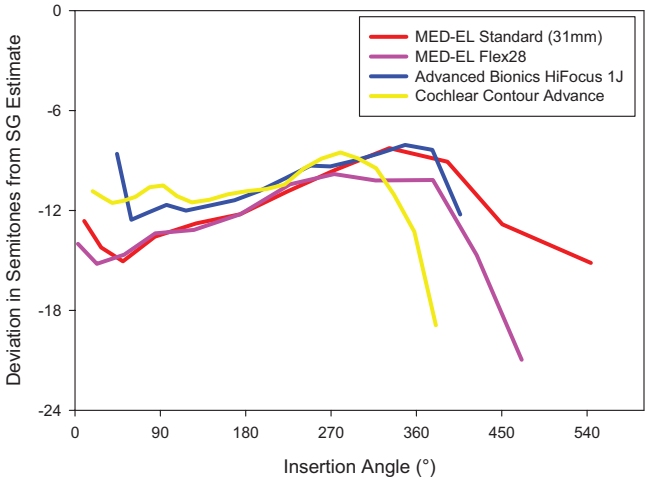

Fig. 5. The deviation in semitones between the frequency delivered to a given angular location and the corresponding frequency as predicted by the spiral ganglion map of Stakhovskaya et al. (2007). Colors of lines are coded by electrode array type.

patient over the long term. Each approach has potential advantages and disadvantages. There is a possible trade-off between deeper insertion and additional cochlear trauma, which may be particularly important in cases where the implanted ear has usable residual hearing. In addition, a deep insertion angle likely should not be sought at the expense of basal stimulation as it reduces speech performance outcomes in that case (e.g., Hochmair et al. 2003; Finley et al. 2008; Sydlowski et al. 2010; Holden et al. 2013). It is worth noting that the surgical point of insertion (i.e., via cochleostomy or RW) will also affect the insertion depth of the electrode array. The second approach, changing the frequency-to-electrode table, can easily be done even in cases of very shallow electrode insertions. The disadvantage of altering the frequency-to-electrode table is that typically adjusting the frequency allocations to match the spiral ganglion map would require reducing the range of frequencies represented by the frequency allocation tables. The last approach is the one that seems to have been adopted by the consensus of CI designers: rely on the human brain's ability to adapt to a modified peripheral mapping. There is a substantial body of work suggesting that humans can indeed show remarkable amounts of auditory adaptation. The first downside is that even though the bulk of this adaptation process takes place within the first few months after implantation, it can sometimes take additional months or years for the process to be complete, and there are also some indications that at least for some listeners the process is not always complete even after extensive experience (Svirsky et al. 2004; Sagi et al. 2010; Reiss et al. 2014).

The MED-EL Standard and Flex28 arrays cover a greater range of the cochlea than the Contour Advance or 1J electrodes, and this allows the MED-EL frequency-to-electrode table to reach down to 100 Hz without a significant departure from the spiral ganglion map curve. In fact, below 650 Hz the curves for the MED-EL arrays are somewhat closer to the spiral ganglion map curve than the other two arrays.

It is worth noting that a correct place pitch match may not be important to achieve. For example, Gani et al. (2007) and Arnoldner et al. (2007) showed that disabling a subset of electrodes near the apex of MED-EL Standard arrays yielded improved performance. By disabling electrodes near the apex, the frequency allocation was shifted away from the spiral ganglion map, suggesting that optimal performance might be obtained for place-frequency allocations away from the spiral ganglion map. Another potential reason for this benefit is that spread of excitation (and therefore channel interaction) might be greater in the apex (Kalkman et al. 2014). If so, apical stimulation would be less precise than stimulation in the middle and basal regions, reducing the need for an accurate frequency-place match. This possibility is supported by the findings that with 31-mm electrodes, some users are able to get good pitch information from all electrodes while others have difficulty discriminating the most apical electrodes (Baumann & Nobbe 2006; Hamzavi & Arnoldner 2006; Gani et al. 2007; Landsberger et al. 2014). Alternatively, an accurate frequency place match might require a current focused stimulation mode (e.g., Landsberger et al. 2012; Fielden et al. 2013; Saoji et al. 2013) in the apex to obtain proper place specificity. Further studies are required to fully assess the clinical significance of the frequency mismatch.

The question arises whether the frequency estimate from Stakhovskaya et al. (2007) is indeed the most relevant place

pitch map for analyzing CI stimulation. One way to address the validity of that frequency-to-place map would be to examine electroacoustic pitch matching studies performed very shortly after initial stimulation, preferably before users have had any experience listening to speech with their implant. Vermeire et al. (2011) pitch matched single electrode pulse trains in one ear to acoustic pure-tones in a normal-hearing contralateral ear with subjects before they had any opportunity to adapt to a speech-processing strategy. Although pitch matches were not significantly different from the spiral ganglion estimate, responses tended to be lower in frequency than predicted by the spiral ganglion map. A similar result was obtained by McDermott et al. (2009), who examined pitch matches on the most apical electrode of Nucleus users who completed the experiment before experiencing any other sounds through their CI. Results from three of five subjects were consistent with the Stakhovskaya et al. map, whereas results for the two other subjects were somewhat lower in frequency than would be predicted by the map. In summary, behavioral data suggest that the Stakhovskaya et al. map may not be perfect but it might be a reasonable first approximation, thus justifying its use in the present analyses.

The present results, together with the existing literature on speech perception by postlingually deafened CI users, suggest that standard placement and programming of most CIs result in a certain amount of frequency mismatch with respect to normal acoustic stimulation of the cochlea. The same literature, however, suggests that the human brain is quite capable of adapting to better deal with such frequency mismatch, at least to some extent. Here, we quantified the approximate intracochlear location of different electrodes and examined it in reference to the default frequency allocation tables used by the corresponding speech processors, and later compared the resulting curves to a reasonable estimate of an acoustic frequency-to-place map in the human cochlea. Perhaps the most remarkable feature of this data set lies in the similarities across manufacturers rather than in the differences. Consider that Figure 4 results from the independent efforts of different electrode design teams (which largely determine positions of the data points along the y axis) and different signal processing teams (which largely determine positions along the x axis) at three different companies, and yet the curves show a remarkable degree of overlap above 650 Hz.

ACKNOWLEDGMENTS

We are grateful to Jonathon Kirk, Laura Holden, and Johan Frijns for providing information on insertion depths measured by other groups that was incorporated in Table 1 and to Susan Waltzman for providing references regarding time to asymptotic speech perception in cochlear implant users. Further references for insertion depths measurements were taken from Table 2 of Boyd (2011). Support for this research was provided by the National Institutes of Health/National Institute on Deafness and Other Communication Disorders (R01 DC012152, PI: Landsberger, and R01 DC03937, PI: Svirsky), a MED-EL Hearing Solutions grant (PI: Landsberger), and Cochlear Corporation (PI: Roland).

Address for correspondence: David M. Landsberger, Department of Otolaryngology, New York University School of Medicine, 550 1st Avenue, STE NBV 5E5, New York, NY 10016, USA. E-mail: David.Landsberger@nyumc.org

Received September 18, 2014; accepted February 13, 2015.

REFERENCES

Adunka, O. F., Pillsbury, H. C., Kiefer, J. (2006). Combining perimodiolar electrode placement and atraumatic insertion properties in cochlear implantation—Fact or fantasy? *Acta Otolaryngol*, *126*, 475–482.

Arnoldner, C., Riss, D., Baumgartner, W. D., et al. (2007). Cochlear implant channel separation and its influence on speech perception—Implications for a new electrode design. *Audiol Neurootol*, *12*, 313–324.

Başkent, D., & Shannon, R. V. (2003). Speech recognition under conditions of frequency-place compression and expansion. *J Acoust Soc Am*, *113*(4 Pt 1), 2064–2076.

Başkent, D., & Shannon, R. V. (2005). Interactions between cochlear implant electrode insertion depth and frequency-place mapping. *J Acoust Soc Am*, *117*(3 Pt 1), 1405–1416.

Baumann, U., & Nobbe, A. (2004). Pitch ranking with deeply inserted electrode arrays. *Ear Hear*, *25*, 275–283.

Baumann, U., & Nobbe, A. (2006). The cochlear implant electrode-pitch function. *Hear Res*, *213*, 34–42.

Boyd, P. J. (2011). Potential benefits from deeply inserted cochlear implant electrodes. *Ear Hear*, *32*, 411–427.

Buchman, C. A., Dillon, M. T., King, E. R., et al. (2014). Influence of cochlear implant insertion depth on performance: A prospective randomized trial. *Otol Neurotol*, *35*, 1773–1779.

Cohen, L. T., Xu, J., Xu, S. A., et al. (1996). Improved and simplified methods for specifying positions of the electrode bands of a cochlear implant array. *Am J Otol*, *17*, 859–865.

Cosetti, M. K., Troob, S. H., Latzman, J. M., et al. (2012). An evidence-based algorithm for intraoperative monitoring during cochlear implantation. *Otol Neurotol*, *33*, 169–176.

Fielden, C. A., Kluk, K., McKay, C. M. (2013). Place specificity of monopolar and tripolar stimuli in cochlear implants: The influence of residual masking. *J Acoust Soc Am*, *133*, 4109–4123.

Finley, C. C., Holden, T. A., Holden, L. K., et al. (2008). Role of electrode placement as a contributor to variability in cochlear implant outcomes. *Otol Neurotol*, *29*, 920–928.

Fitzgerald, M. B., Sagi, E., Jackson, M., et al. (2008). Reimplantation of hybrid cochlear implant users with a full-length electrode after loss of residual hearing. *Otol Neurotol*, *29*, 168–173.

Fraysse, B., Macias, A. R., Sterkers, O., et al. (2006). Residual hearing conservation and electroacoustic stimulation with the nucleus 24 contour advance cochlear implant. *Otol Neurotol*, *27*, 624–633.

Fu, Q. J., & Shannon, R. V. (1999). Recognition of spectrally degraded and frequency-shifted vowels in acoustic and electric hearing. *J Acoust Soc Am*, *105*, 1889–1900.

Gani, M., Valentini, G., Sigrist, A., et al. (2007). Implications of deep electrode insertion on cochlear implant fitting. *J Assoc Res Otolaryngol*, *8*, 69–83.

Greenwood, D. D. (1961). Critical bandwidth and the frequency coordinates of the basilar membrane. *J Acoust Soc Am*, *33*, 1344–1356.

Hamzavi, J., & Arnoldner, C. (2006). Effect of deep insertion of the cochlear implant electrode array on pitch estimation and speech perception. *Acta Otolaryngol*, *126*, 1182–1187.

Hamzavi, J., Baumgartner, W. D., Pok, S. M., et al. (2003). Variables affecting speech perception in postlingually deaf adults following cochlear implantation. *Acta Otolaryngol*, *123*, 493–498.

Hochmair, I., Arnold, W., Nopp, P., et al. (2003). Deep electrode insertion in cochlear implants: Apical morphology, electrodes and speech perception results. *Acta Otolaryngol*, *123*, 612–617.

Holden, L. K., Finley, C. C., Firszt, J. B., et al. (2013). Factors affecting open-set word recognition in adults with cochlear implants. *Ear Hear*, *34*, 342–360.

Kalkman, R. K., Briaire, J. J., Dekker, D. M., et al. (2014). Place pitch versus electrode location in a realistic computational model of the implanted human cochlea. *Hear Res*, *315*, 10–24.

Kós, M. I., Boëx, C., Sigrist, A., et al. (2005). Measurements of electrode position inside the cochlea for different cochlear implant systems. *Acta Otolaryngol*, *125*, 474–480.

Landsberger, D. M., Mertens, G., Punte, A. K., et al. (2014). Perceptual changes in place of stimulation with long cochlear implant electrode arrays. *J Acoust Soc Am*, *135*, EL75–EL81.

Landsberger, D. M., Padilla, M., Srinivasan, A. G. (2012). Reducing current spread using current focusing in cochlear implant users. *Hear Res*, *284*, 16–24.

Li, T., & Fu, Q. J. (2010). Effects of spectral shifting on speech perception in noise. *Hear Res*, *270*, 81–88.

Marsh, M. A., Xu, J., Blamey, P. J., et al. (1993). Radiologic evaluation of multichannel intracochlear implant insertion depth. *Am J Otol*, *14*, 386–391.

McDermott, H., Sucher, C., Simpson, A. (2009). Electro-acoustic stimulation. Acoustic and electric pitch comparisons. *Audiol Neurootol*, *14*(Suppl 1), 2–7.

Radeloff, A., Mack, M., Baghi, M., et al. (2008). Variance of angular insertion depths in free-fitting and perimodiolar cochlear implant electrodes. *Otol Neurotol*, *29*, 131–136.

Reiss, L. A., Turner, C. W., Erenberg, S. R., et al. (2007). Changes in pitch with a cochlear implant over time. *J Assoc Res Otolaryngol*, *8*, 241–257.

Reiss, L. A., Turner, C. W., Karsten, S. A., et al. (2014). Plasticity in human pitch perception induced by tonotopically mismatched electro-acoustic stimulation. *Neuroscience*, *256*, 43–52.

Ruffin, C. V., Tyler, R. S., Witt, S. A., et al. (2007). Long-term performance of Clarion 1.0 cochlear implant users. *Laryngoscope*, *117*, 1183–1190.

Sagi, E., Fu, Q. J., Galvin, J. J. III, et al. (2010). A model of incomplete adaptation to a severely shifted frequency-to-electrode mapping by cochlear implant users. *J Assoc Res Otolaryngol*, *11*, 69–78.

Saoji, A. A., Landsberger, D. M., Padilla, M., et al. (2013). Masking patterns for monopolar and phantom electrode stimulation in cochlear implants. *Hear Res*, *298*, 109–116.

Stakhovskaya, O., Sridhar, D., Bonham, B. H., et al. (2007). Frequency map for the human cochlear spiral ganglion: Implications for cochlear implants. *J Assoc Res Otolaryngol*, *8*, 220–233.

Svirsky, M. A., Silveira, A., Neuburger, H., et al. (2004). Long-term auditory adaptation to a modified peripheral frequency map. *Acta Otolaryngol*, *124*, 381–386.

Svirsky, M. A., Silveira, A., Suarez, H., et al. (2001). Auditory learning and adaptation after cochlear implantation: A preliminary study of discrimination and labeling of vowel sounds by cochlear implant users. *Acta Otolaryngol*, *121*, 262–265.

Sydlowski, S. A., Oakley, S. R., Borton, S. A., et al. (2010). Negative effect of deep cochlear implant electrode insertion on speech perception. *Cochlear Implants Int*, *11*, 233–240.

Trieger, A., Schulze, A., Schneider, M., et al. (2011). *In vivo* measurements of the insertion depth of cochlear implant arrays using flat-panel volume computed tomography. *Otol Neurotol*, *32*, 152–157.

Tyler, R. S., Parkinson, A. J., Woodworth, G. G., et al. (1997). Performance over time of adult patients using the Ineraid or nucleus cochlear implant. *J Acoust Soc Am*, *102*, 508–522.

van der Marel, K. S., Briaire, J. J., Wolterbeek, R., et al. (2014). Diversity in cochlear morphology and its influence on cochlear implant electrode position. *Ear Hear*, *35*, e9–e20.

Vermeire, K., Kleine Punte, A., Schatzer, R., et al. (2011). Frequency-place map for electrical stimulation in cochlear implants: Change over time. In *Conference on Implantable Auditory Prostheses*. Asilomar Conference Grounds, Pacific Grove, CA, USA.

Vermeire, K., Nobbe, A., Schleich, P., et al. (2008). Neural tonotopy in cochlear implants: An evaluation in unilateral cochlear implant patients with unilateral deafness and tinnitus. *Hear Res*, *245*, 98–106.

Xu, J., Xu, S. A., Cohen, L. T., et al. (2000). Cochlear view: Postoperative radiography for cochlear implantation. *Am J Otol*, *21*, 49–56.

REFERENCE NOTE

1. Holden, L. K. (2014). Personal communication.